Received: 29 August 2018 | Revised: 16 November 2018 | Accepted: 7 December 2018

DOI: 10.1111/cbdd.13462

RESEARCH LETTER

WILEY

Docking simulation and antibiotic discovery targeting the MlaC protein in Gram-negative bacteria

Yu-ming M. Huang[1] | **Jason Munguia**[2] | **Yinglong Miao**[3] | **Victor Nizet**[2,4] | **J. Andrew McCammon**[1,3]

[1]Department of Pharmacology, University of California, San Diego, La Jolla, California

[2]Department of Pediatrics, University of California, San Diego, La Jolla, California

[3]Department of Chemistry and Biochemistry, University of California, San Diego, La Jolla, California

[4]Skaggs School of Pharmacy and Pharmaceutical Sciences, University of California, San Diego, La Jolla, California

Correspondence
Yu-ming M. Huang, Department of Pharmacology, University of California, San Diego, La Jolla, CA.
Email: yuh155@ucsd.edu

Present address
Yinglong Miao, Department of Molecular Biosciences, Center for Computational Biology, University of Kansas, Lawrence, Kansas

Funding information
NIH NBCR, Grant/Award Number: GM103426; NIH, Grant/Award Number: GM31749; NSF, Grant/Award Number: 1020765

Abstract

To maintain the lipid asymmetry of the cell envelope in Gram-negative bacteria, the MlaC protein serves as a lipid transfer factor and delivers phospholipids from the outer to the inner membrane. A strategy of antibiotic discovery is to design a proper compound that can tightly bind to the MlaC protein and inhibit the MlaC function. In this study, we performed virtual screening on multiple MlaC structures obtained from molecular dynamics simulations to identify potential MlaC binders. Our results suggested that clorobiocin is a compound that could bind to the MlaC protein. Through the comparison of the bound geometry between clorobiocin and novobiocin, we pointed out that the methyl-pyrrole group of the noviose sugar in clorobiocin forms hydrophobic interactions with amino acids in the phospholipid binding pocket, which allows the compound to bind deep in the active site. This also explains why clorobiocin shows a tighter binding affinity than novobiocin. Our study highlights a practical path of antibiotic development against Gram-negative bacteria.

KEYWORDS

antibiotic, drug design, MlaC protein, virtual screening

1 | INTRODUCTION

The outer membrane of Gram-negative bacteria has an asymmetric structure with lipopolysaccharides at the outer leaflet and phospholipids at the inner leaflet (Kamio & Nikaido, 1976). To maintain this lipid asymmetry, the Mla pathway, an ATP-binding cassette transport system, can transfer misplaced phospholipids from the outer to the inner membrane (Malinverni & Silhavy, 2009; Munguia et al., 2017; Narita, 2011). By inhibiting this fundamental mechanism, a strategy of antibiotic discovery is to design a small molecule that can tightly bind to the MlaC protein, a key element in the Mla pathway, and interrupt the phospholipid transport on the membranes further limiting the bacteria's capacity to cause disease. This work aims to look for potential inhibitors of the MlaC protein through computational modeling.

A crystal structure of MlaC–phospholipid complex from *Ralstonia solanacearum* showed that the protein is folded into nine alpha helices and five beta strands (Figure 1). The MlaC protein from *Acinetobacter baumannii* was built by homology modeling. Through performing molecular dynamics (MD) simulations, the dynamic properties of the MlaC protein in

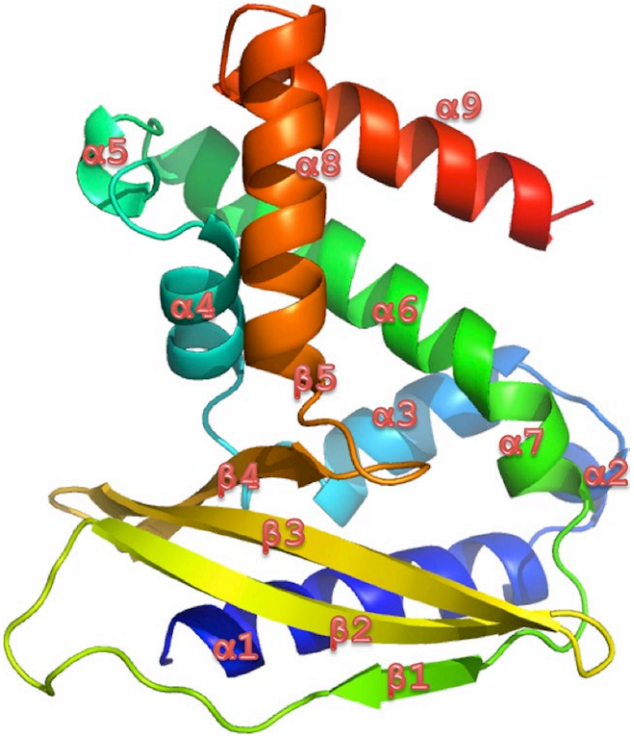

FIGURE 1 Structure of the MlaC protein

both apo- and phospholipid-bound state from the two bacteria sources have been investigated (Huang et al., 2016). The simulations revealed multiple protein conformations with different binding pocket volumes, which may directly contribute to the design of antibiotics of the MlaC protein (Huang et al., 2016).

Virtual screening has been widely applied in structure-based drug design. These approaches are now well established in a step-by-step process, including refinements of protein structure, calculations of ligand binding thermodynamics, ranking compounds, and predicting binding poses (Amaro et al., 2018). The early docking studies were successful in antiviral discovery for HIV and influenza with a rigid protein–ligand model (Kaldor et al., 1997; Vonitzstein et al., 1993). Later on, the docking protocol allowed a flexible model of receptor and substrate, continuing to improve the success in drug discovery (Rosenfeld, Vajda, & Delisi, 1995). Thus, in this work, we performed both rigid and flexible docking to identify new inhibitors of the MlaC protein with potential antibiotic activity for Gram-negative bacteria.

2 | METHODS AND MATERIALS

2.1 | MlaC protein structure preparation

The structure of the MlaC protein from *Acinetobacter baumannii* was built according to the MlaC–phospholipid complex from *Ralstonia solanacearum* (PDB ID: 2QGU) through the homology modeling tools on the i-TASSER server (Yang et al., 2015). The sequence identity between the two MlaC proteins from different species has been explored in detail from the early MlaC dynamic study (Huang et al., 2016). Following the MD protocol from the study (Huang et al., 2016), we performed 100-ns MD simulations on the MlaC protein from *Acinetobacter baumannii* using the Amber 14 package (Case et al., 2005; Salomon-Ferrer, Case, & Walker, 2013). The g-cluster program in Gromacs 4.5.5 package (Lange & Grubmuller, 2006) was applied to cluster the MD trajectory into 30 clusters based on the root-mean-square deviation of the protein backbone. The major conformations from the 30 clusters were used for the following screening simulations, following the relaxed complex scheme (Amaro, Baron, & McCammon, 2008; Lin, Perryman, Schames, & McCammon, 2002, 2003).

2.2 | Virtual screening

Virtual screening of the MlaC protein was performed with the virtual screening workflow in Schrodinger Suite 2016 (Friesner et al., 2004; Halgren et al., 2004). The workflow includes ligand preparation using LigPrep, filtration using propfilter on QikProp properties, and Glide docking at the three accuracy levels, including the high-throughput virtual screening (HTVS), standard precision (SP), and extra precision (XP) (Friesner et al., 2006). The National Cancer Institute (NCI) diversity set IV, which contains 1,596 compounds, was used as a screening library. First, the ligands were prepared using LigPrep with the OPLS2005 force field. Before running the workflow, we generated Glide grids for a receptor with the center located at the MlaC phospholipid binding site. The inner and outer boxes for docking were set to 10 and 27 Å, respectively. Then, the HTVS, SP, and XP docking were carried out.

2.3 | Induced-fit docking

We performed induced-fit docking using Glide in Schrodinger Suite 2016 (Friesner et al., 2004, 2006; Halgren et al., 2004). Two ligands, clorobiocin and novobiocin, were docked to five different MlaC structures, for which the protein conformations were generated by clustering the trajectory from the earlier MD simulations (Huang et al., 2016). We set the phospholipid binding site of MlaC protein as the docking center. The inner docking box was set to 10 Å, and the Glide default was used for the outer box value. The MlaC protein was rigid during the docking simulations except for the residues within 5 Å of the docking center.

2.4 | Experimental methods

Checkerboards were performed in RPMI 1640 (Gibco) supplemented with 5% Luria–Bertani broth (BD Difco). *A. baumannii* AB5075 was grown to mid-log phase in LB broth, washed twice with PBS, and suspended to a concentration of 5×10^6 cfu/ml in RPMI + 5% LB. Clorobiocin was prepared in a range of 500–7.8 μM and the antimicrobial peptide LL-37 in a range of 80–1.25 μM. Ten microliters of diluted range LL-37 was added across eight columns in a 96-well plate containing 70 μl of RPMI + 5% LB, followed by 10 μl of clorobiocin dilution range down the rows. Ten microliters of bacteria was then added and placed at 37°C overnight. Final concentrations were 50–0.78 μM clorobiocin, 8–0.125 μM LL-37, and 5×10^5 cfu/ml *A. baumannii*. Plates were read by eye, and data were analyzed. Fractional inhibitory concentration (FIC) was calculated using following formula:

$$\mathrm{FIC} = \Sigma \frac{\mathrm{Conc.clorobiocin}}{\mathrm{MIC\,clorobiocin}} + \frac{\mathrm{Conc.\,LL{-}37}}{\mathrm{MIC\,LL{-}37}}$$

3 | RESULTS AND DISCUSSION

3.1 | In silico screen to select potential MlaC inhibitors

We performed a computational technique, virtual screening, and docking simulation, to identify potential MlaC inhibitors. The methods have been broadly applied in drug discovery through searching libraries of small molecules to identify candidate compounds that bind to a target protein (Joshi et al., 2017; Miao et al., 2016; Singh & Coumar, 2017). We first used the 30 protein conformations clustered from the MD simulations as receptor templates to perform virtual screening. For each conformational cluster, through the docking of ~1,600 compounds of the NCI library, we identified 120–150 compounds that show the lowest binding free energy score sorted by the screening. According to the docking score of each simulation, we listed the 20 compounds that have a preferred binding affinity to the MlaC protein in Table 1. Then, we performed experimental checkerboards to carefully examine these 20 compounds. One of the compounds, clorobiocin (NCI compound number 227186), was noticed to play an active role in the interference of Mla pathways. When clorobiocin was tested in an *A. baumannii* checkerboard with the human antimicrobial peptide LL-37, Figure 2 shows synergistic effects (FIC = 0.5 at concentration of 12.5 μM clorobiocin and 1 μM LL-37). This result implied potential interactions with the Mla pathway. Thus, we continued to learn molecular insights into the binding generated between the MlaC protein and clorobiocin.

TABLE 1 List of the 20 compounds from the NCI library with the best docking scores to the MlaC protein

Ranking	NCI compound number	Binding energy (kcal/mol)
1	268251	−13.53
2	354844	−13.50
3	227186	−13.14
4	345647	−13.12
5	37553	−12.90
6	122819	−12.48
7	89821	−12.37
8	91397	−12.08
9	111210	−12.08
10	128606	−12.05
11	84100	−11.96
12	335504	−11.83
13	275266	−11.79
14	309892	−11.75
15	9037	−11.74
16	163443	−11.69
17	80997	−11.69
18	654260	−11.64
19	186200	−11.63
20	156565	−11.61

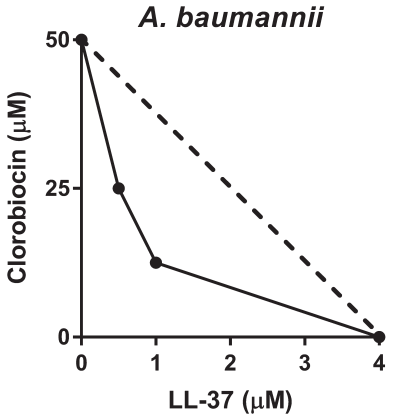

FIGURE 2 Experimental measurements of FIC change between clorobiocin and LL-37 concentrations

3.2 | Comparison between clorobiocin and novobiocin

Novobiocin is structurally similar to clorobiocin. It has been known as an agent for the treatment of resistant bacterial

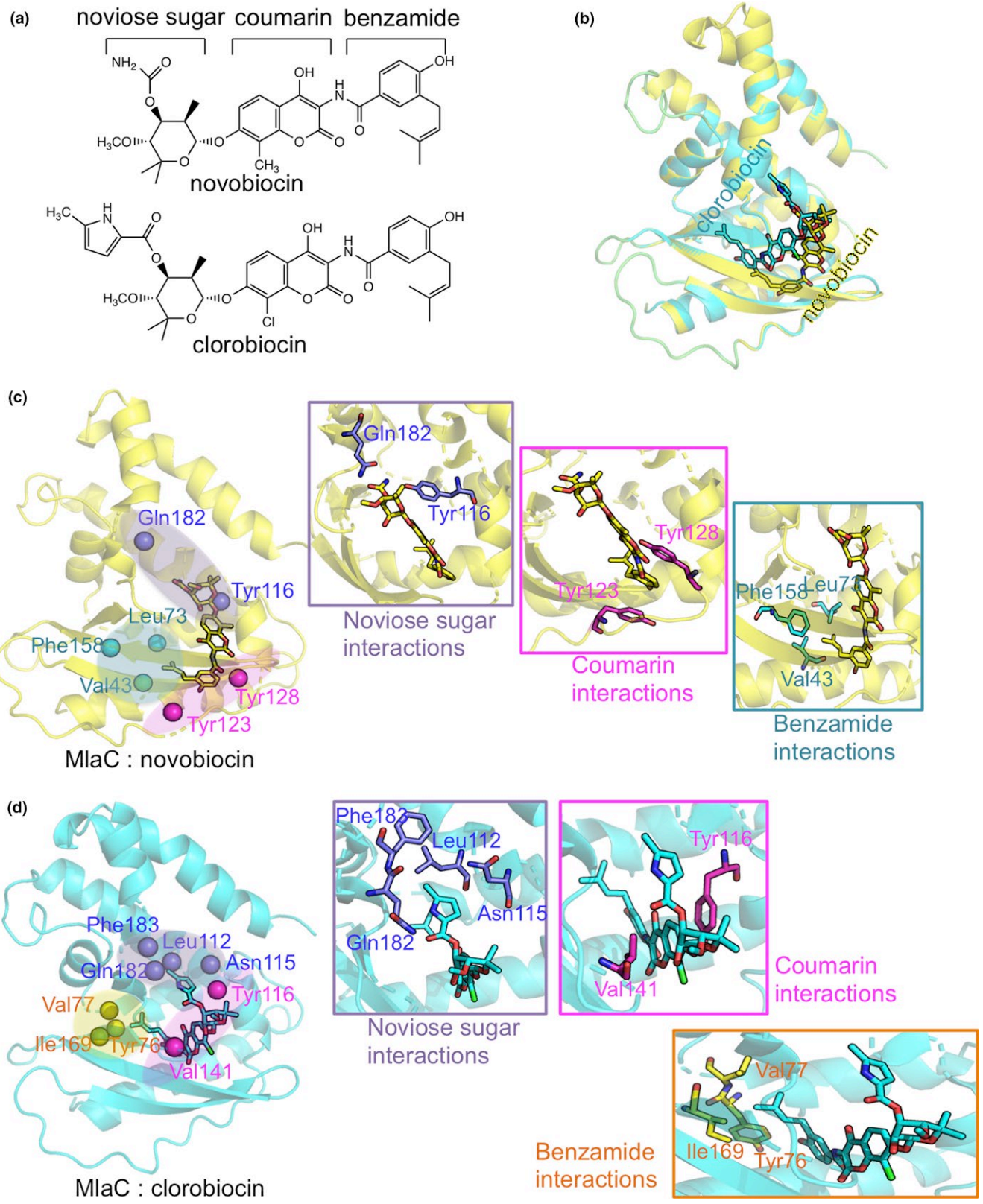

FIGURE 3 (a) Chemical structures of novobiocin and clorobiocin. (b) Structural alignment of novobiocin (yellow) and clorobiocin (cyan) complexes reported from induced-fit docking simulations. (c) Structure of MlaC–novobiocin complex reported from induced-fit docking calculations. Bond representations of cyan, magenta, and purple color indicate that the protein residues form interactions with the isobutylene functional group on benzamide, the benzamide group, and the amine group of noviose sugar, respectively. (d) Structure of MlaC–clorobiocin complex reported from induced-fit docking simulations. Bond representations of yellow, magenta, and purple color indicate that the residues form interactions with the isobutylene group of clorobiocin, the center coumarin group, and the methyl-pyrrole group of noviose sugar, respectively

TABLE 2 The docking scores reported from Schrodinger Suite of clorobiocin and novobiocin binding to five different conformations of MlaC protein

MlaC protein conformation	Novobiocin (kcal/mol)	Clorobiocin (kcal/mol)
Conformation 1	−12.375	−12.826
Conformation 2	−10.229	−11.539
Conformation 3	−10.328	−11.218
Conformation 4	−11.648	−11.522
Conformation 5	−10.076	−10.855

infections since the 1950s (Bisacchi & Manchester, 2015). Both novobiocin and clorobiocin are composed of three chemical segments: noviose sugar, coumarin, and benzamide group (see Figure 3a). The only two structural differences between novobiocin and clorobiocin are (1) the functional group at noviose sugar and (2) the replacement of chloride by a methyl group at coumarin. Although earlier studies showed that novobiocin is effective in antibacterial therapy, our experimental investigation does not show it alters the bacterial activity involving Mla mechanisms; however, clorobiocin does. Thus, this prompted us to study why the slight structural differences between novobiocin and clorobiocin could result in different behaviors in antibiotics.

We performed induced-fit docking of novobiocin and clorobiocin to five different MlaC conformations to explore ligand–protein binding geometries of the MlaC systems. Compared to conventional docking tools with a rigid protein coordinate, the induced-fit protocol here allows conformational changes in the receptor binding site induced by a bound ligand, which enables us to quickly predict active site geometries with minimal expense. Our results show that the best docking scores of novobiocin and clorobiocin binding to the MlaC protein are −12.38 and −12.83 kcal/mol, respectively (Table 2). Both bound poses of novobiocin and clorobiocin from docking simulations demonstrate that the benzamide group points toward the active site, while the noviose sugar is exposed to solvent and tends to interact with the protein residues near the entrance of the lipid binding site (Figure 3b). The structural alignment of novobiocin and clorobiocin shows that clorobiocin could be placed deeper in the binding pocket, and the ligand geometry of clorobiocin fits better to MlaC protein conformation than novobiocin (Figure 3b), which may explain why clorobiocin could bind tighter than novobiocin to MlaC.

We then examined closely the detailed interactions between the ligands and MlaC protein. Three major contacts are formed between novobiocin and the MlaC: First, the isobutylene functional group on benzamide interacts with the hydrophobic residues, Val43, Leu-73, and Phe158 (Figure 3c, benzamide interactions); second, the benzamide group displays pi–pi stacking with Tyr123 and Tyr128, which allows binding of the compound in the protein pocket (Figure 3c, coumarin interactions); and third, the amine group of noviose sugar forms polar interactions with Tyr116 and Gln182 (Figure 3c, noviose sugar interactions). Compared to novobiocin, the isobutylene group of clorobiocin binds deeper in the binding pocket, interacting with Tyr76, Val77, and Ile169 (Figure 3d, benzamide interactions). The center coumarin group is clamped between Tyr116 and Val141 by non-polar interactions (Figure 3d, coumarin interactions). Importantly, the methyl-pyrrole group of noviose sugar in clorobiocin binds nicely at the hydrophobic pocket formed by Leu-112, Asn115, Gln182, and Phe183 (Figure 3d, noviose sugar interactions). Apparently, the replacement of amide from novobiocin to methyl-pyrrole group in clorobiocin enables the ligand to form more contacts with the MlaC protein and further increases the binding affinity.

ACKNOWLEDGMENTS

This work was supported by the NIH, NBCR, and NSF supercomputer centers.

ORCID

Yu-ming M. Huang https://orcid.org/0000-0003-3257-6170

REFERENCES

Amaro, R. E., Baron, R., & McCammon, J. A. (2008). An improved relaxed complex scheme for receptor flexibility in computer-aided drug design. *Journal of Computer-Aided Molecular Design*, *22*, 693–705. https://doi.org/10.1007/s10822-007-9159-2

Amaro, R. E., Baudry, J., Chodera, J., Demir, O., McCammon, J. A., Miao, Y. L., & Smith, J. C. (2018). Ensemble docking in drug discovery. *Biophysical Journal*, *114*, 2271–2278. https://doi.org/10.1016/j.bpj.2018.02.038

Bisacchi, G. S., & Manchester, J. I. (2015). A new-class antibacterial-almost. Lessons in drug discovery and development: A critical analysis of more than 50 years of effort toward ATPase inhibitors of DNA gyrase and topoisomerase IV. *ACS Infectious Diseases*, *1*, 4–41. https://doi.org/10.1021/id500013t

Case, D. A., Cheatham, T. E. III, Darden, T., Gohlke, H., Luo, R., Merz, K. M. Jr., … Woods, R. J. (2005). The Amber biomolecular simulation programs. *Journal of Computational Chemistry*, *26*, 1668–1688. https://doi.org/10.1002/(ISSN)1096-987X

Friesner, R. A., Banks, J. L., Murphy, R. B., Halgren, T. A., Klicic, J. J., Mainz, D. T., … Shenkin, P. S. (2004). Glide: A new approach for rapid, accurate docking and scoring. 1. Method and assessment of docking accuracy. *Journal of Medicinal Chemistry*, *47*, 1739–1749. https://doi.org/10.1021/jm0306430

Friesner, R. A., Murphy, R. B., Repasky, M. P., Frye, L. L., Greenwood, J. R., Halgren, T. A., … Mainz, D. T. (2006). Extra precision glide: Docking and scoring incorporating a model of hydrophobic enclosure for protein-ligand complexes. *Journal of Medicinal Chemistry*, *49*, 6177–6196. https://doi.org/10.1021/jm051256o

Halgren, T. A., Murphy, R. B., Friesner, R. A., Beard, H. S., Frye, L. L., Pollard, W. T., & Banks, J. L. (2004). Glide: A new approach for rapid, accurate docking and scoring. 2. Enrichment factors in database screening. *Journal of Medicinal Chemistry*, *47*, 1750–1759. https://doi.org/10.1021/jm030644s

Huang, Y. M., Miao, Y. L., Munguia, J., Lin, L., Nizet, V., & McCammon, J. A. (2016). Molecular dynamic study of MlaC protein in Gram-negative bacteria: Conformational flexibility, solvent effect and protein-phospholipid binding. *Protein Science*, *25*, 1430–1437. https://doi.org/10.1002/pro.2939

Joshi, P., McCann, G. J. P., Sonawane, V. R., Vishwakarma, R. A., Chaudhuri, B., & Bharate, S. B. (2017). Identification of potent and selective CYP1A1 inhibitors via combined ligand and structure-based virtual screening and their in vitro validation in sacchrosomes and live human cells. *Journal of Chemical Information and Modeling*, *57*, 1309–1320. https://doi.org/10.1021/acs.jcim.7b00095

Kaldor, S. W., Kalish, V. J., Davies, J. F. II, Shetty, B. V., Fritz, J. E., Appelt, K., … Tatlock, J. H. (1997). Viracept (nelfinavir mesylate, AG1343): A potent, orally bioavailable inhibitor of HIV-1 protease. *Journal of Medicinal Chemistry*, *40*, 3979–3985. https://doi.org/10.1021/jm9704098

Kamio, Y., & Nikaido, H. (1976). Outer membrane of *Salmonella typhimurium*: Accessibility of phospholipid head groups to phospholipase c and cyanogen bromide activated dextran in the external medium. *Biochemistry*, *15*, 2561–2570. https://doi.org/10.1021/bi00657a012

Lange, O. F., & Grubmuller, H. (2006). Generalized correlation for biomolecular dynamics. *Proteins*, *62*, 1053–1061.

Lin, J. H., Perryman, A. L., Schames, J. R., & McCammon, J. A. (2002). Computational drug design accommodating receptor flexibility: The relaxed complex scheme. *Journal of the American Chemical Society*, *124*, 5632–5633. https://doi.org/10.1021/ja0260162

Lin, J. H., Perryman, A. L., Schames, J. R., & McCammon, J. A. (2003). The relaxed complex method: Accommodating receptor flexibility for drug design with an improved scoring scheme. *Biopolymers*, *68*, 47–62. https://doi.org/10.1002/(ISSN)1097-0282

Malinverni, J. C., & Silhavy, T. J. (2009). An ABC transport system that maintains lipid asymmetry in the gram-negative outer membrane. *Proceedings of the National Academy of Sciences of the United States of America*, *106*, 8009–8014. https://doi.org/10.1073/pnas.0903229106

Miao, Y. L., Goldfeld, D. A., Von Moo, E., Sexton, P. M., Christopoulos, A., McCammon, J. A., & Valant, C. (2016). Accelerated structure-based design of chemically diverse allosteric modulators of a muscarinic G protein-coupled receptor. *Proceedings of the National Academy of Sciences of the United States of America*, *113*, E5675–E5684. https://doi.org/10.1073/pnas.1612353113

Munguia, J., LaRock, D. L., Tsunemoto, H., Olson, J., Cornax, I., Pogliano, J., & Nizet, V. (2017). The Mla pathway is critical for Pseudomonas aeruginosa resistance to outer membrane permeabilization and host innate immune clearance. *Journal of Molecular Medicine*, *95*, 1127–1136. https://doi.org/10.1007/s00109-017-1579-4

Narita, S. (2011). ABC transporters involved in the biogenesis of the outer membrane in gram-negative bacteria. *Bioscience, Biotechnology, and Biochemistry*, *75*, 1044–1054. https://doi.org/10.1271/bbb.110115

Rosenfeld, R., Vajda, S., & Delisi, C. (1995). Flexible docking and design. *Annual Review of Biophysics and Biomolecular Structure*, *24*, 677–700. https://doi.org/10.1146/annurev.bb.24.060195.003333

Salomon-Ferrer, R., Case, D. A., & Walker, R. C. (2013). An overview of the Amber biomolecular simulation package. *WIREs Computational Molecular Science*, *3*, 198. https://doi.org/10.1002/wcms.1121

Singh, V. K., & Coumar, M. S. (2017). Ensemble-based virtual screening: Identification of a potential allosteric inhibitor of Bcr-Abl. *Journal of Molecular Modeling*, *23*, 218. https://doi.org/10.1007/s00894-017-3384-y

Vonitzstein, M., Wu, W. Y., Kok, G. B., Pegg, M. S., Dyason, J. C., Jin, B., et al. (1993). Rational design of potent sialidase-based inhibitors of influenza virus replication. *Nature*, *363*, 418–423. https://doi.org/10.1038/363418a0

Yang, J., Yan, R., Roy, A., Xu, D., Poisson, J., & Zhang, Y. (2015). The I-TASSER Suite: Protein structure and function prediction. *Nature Methods*, *12*, 7–8. https://doi.org/10.1038/nmeth.3213

How to cite this article: Huang Y-MM, Munguia J, Miao Y, Nizet V, McCammon JA. Docking simulation and antibiotic discovery targeting the MlaC protein in Gram-negative bacteria. *Chem Biol Drug Des*. 2019;00:1–6. https://doi.org/10.1111/cbdd.13462